ELSEVIER

Surface and Coatings Technology 133–134 (2000) 101–105

SURFACE & COATINGS TECHNOLOGY

www.elsevier.nl/locate/surfcoat

Effect of transverse current injection during vacuum arc deposition of TiN

N. Parkansky[a,*], V. Zhitomirsky[a], B. Alterkop[a], S. Goldsmith[a], R.L. Boxman[a], Yu. Rosenberg[b], Z. Barkay[b]

[a] *Electrical Discharge and Plasma Laboratory, Tel Aviv University, P.O. Box 39040, Tel Aviv 69978, Israel*
[b] *Wolfson Center for Material Research, Tel Aviv University, P.O. Box 39040, Tel Aviv 69978, Israel*

Abstract

Transverse current injection (TCI) is a technique in which an electrical current is imposed parallel to the surface of a workpiece exposed to processing or to a service environment. In this work, TCI was applied during vacuum arc deposition of TiN film on WC cemented carbide substrates (90% WC, 8% Co, 2% TaNbC). Bar samples with dimensions $5 \times 6.5 \times 20$ mm were mounted on a holder that provided electrical contacts at their ends, and a thermocouple to measure sample temperature. Prior to deposition, the substrates were heated in vacuum up to 150°C by a current of 100 A. The TiN coatings were obtained by vacuum arc deposition of Ti plasma in a 0.67-Pa nitrogen background. Films with different thickness were obtained by controlling of the plasma flow density. The arc current was 250 A, and substrate temperature during deposition was in the range 110–130°C. Two deposition rates,: 2.3–3 and 20–23 nm/s were used. The injected d.c. transverse current was in the range 0–40 A. Surface microhardness was measured by Vickers microindentation using a 25-g load. Film structure was examined by X-ray diffractometry (XRD), scanning electron microscopy (SEM) using scattered electrons (SE), back scattered electrons (BSE), and energy dispersive spectroscopy (EDS). EDS spectra indicated that approximately the same ratio of Ti and N atoms existed both in thick (4–4.5 μm) and in thinner films (~ 0.4 μm). XRD patterns indicated a cubic NaCl-type TiN phase in the thick films, while this phase was absent in the thinner films. In comparison with films deposited without TCI, the maximum microhardness of thick TiN films (~ 4 μm) was larger by a factor of 1.3 with 10 A of transverse current, whereas the maximum microhardness of thinner films (~ 0.4 μm) was up to a factor of 1.7 larger with 20 A of transverse current. TiN coatings deposited at 110–130°C with TCI were uniform and did not contain delaminating fragments, whereas coating deposited using the same deposition parameters but without TCI contained delaminating fragments.

Keywords: Transverse current injection; Vacuum arc deposition; Titanium nitride

1. Introduction

Hard coatings are applied to the surfaces of mechanical components subjected to wear in order to increase their performance or extend their useful life. One application of particular importance is hard coatings for cutting tools such as drills, end mills and lathe inserts. Coatings of hard materials such as TiN have been shown to considerably improve the service life of these tools [1,2]. TiN and related coatings such as ZrN, TiC, (Ti,Al)N, Ti(C,N), as well as diamond and amorphous diamond-like carbon (DLC) can be applied by various techniques, most of which are chemical vapour deposition (CVD) or physical vapour deposition (PVD) [1–3].

The coating hardness, along with other characteristics including the adhesion of the coating to the sub-

* Corresponding author. Tel.: +972-3-640-8176; fax: +972-3-641-0189.
E-mail address: naump@eng.tau.ac.il (N. Parkansky).

0257-8972/00/$ - see front matter
PII: S0257-8972(00)00882-3

strate, the substrate temperature, the chemical and metallurgical stability (including resistance to interdiffusion) of the coating in the wear environment, together determine the performance and service lifetime of the coating. One concern is the temperature of the substrate. In many applications, a lower substrate temperature is desired, either to reduce thermal stress in the coating, or because the substrate cannot tolerate high temperature. Some techniques require high temperatures. Generally, the sample must be heated either through the deposition process, or via external means. Substrate temperatures of 200–600°C are typically used for TiN coating deposition [4,5]. In particular, high substrate temperatures (e.g. 400°C) are employed for industrial TiN deposition on cutting tool substrates to obtain good coating adhesion and tool performance [1,2]. A technique consisting of a cathodic arc source of ions with combination of a low-voltage bias with a high-voltage pulse imposed to a substrate was developed for low-temperature (150°C) TiN coating of low alloy steel and aluminium [6,7]. There is no information on low-temperature TiN coating of cemented carbide substrates. Recently, a technique for improving coating properties in which an electrical field is imposed parallel to the surface of a workpiece during deposition was developed [8–10]. In this transverse current injection (TCI) technique, an electrical current is injected when the processed material is electrically conductive. Generally, the current density is sufficiently low ($< 10^2$ A/cm^2) so that the workpiece heating is not significant [8,9]. It was shown that TCI affects the thin film structure, morphology and electrical conductivity both in the initial and later stages of deposition [9,10]. TCI increases film adhesion on the plastic surface [11], and affects the surface mechanical properties of a cemented carbide [12]. However, the influences of TCI on the mechanical properties of a hard coating on cemented carbide have not been studied yet. In the presented paper, the effects of TCI on the deposition at low temperature of hard TiN coating on cemented carbide substrates and on the properties of the deposited films were studied.

2. Experimental details

The basic scheme of the experiment is presented in Fig. 1. A WC based cemented carbide (90% WC, 8% Co, 2% TaNbC) bar substrate with dimensions of $5 \times 6.5 \times 20$ mm was mounted on a substrate holder which provided electrical contacts at the substrate ends, and a thermocouple for measuring temperature. The holder with substrate was positioned in the deposition chamber of a triple-cathode vacuum arc deposition apparatus described in detail previously [3,11]. In this apparatus, three cathodes of 54-mm diameter were equally

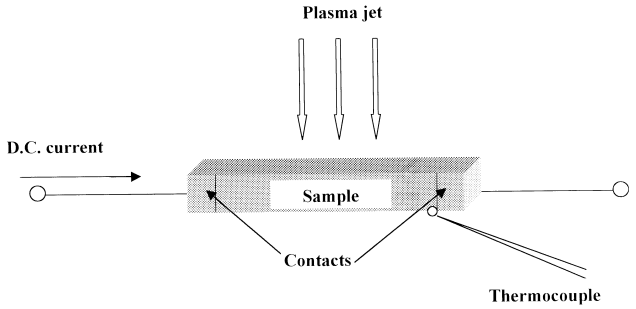

Fig. 1. Schematic diagram of the experimental set-up.

spaced on a 100-mm diameter circle on the cathode plane. A Ti (99.9%) cathode used in the present study was mounted at one of the positions. A d.c. arc discharge of 250 A was applied between the cathode and an annular Cu anode. The anode was grounded, the cathode was connected to the negative terminal of an arc welder power supply, the plasma duct was floating, and the TCI holder contacts were electrically insulated from the chamber and other parts of the deposition system. The plasma jet produced by the cathode spots passed through the anode aperture, entered into a straight plasma duct, in which a 10 mT axial magnetic field was imposed and flowed to the substrate. The substrate was centred on the duct axis, and the distance from the substrate surface to the cathode plane was 560 mm. As the cathode was displaced from the apparatus axis, two beam steering coils were applied [11] to center the beam on the substrate. The system was also equipped with a system for introducing and regulating the flow of the nitrogen gas into the vacuum chamber. The vacuum chamber was sealed, and evacuated to a base pressure of approximately 6.7 mPa. Thereafter, a direct current of 100 A was applied via the electrical contacts in order to heat the substrate. The temperature was monitored with a thermocouple. The heating was terminated when the temperature reached 150°C. Then a 250-A vacuum arc was ignited between the Ti cathode and the anode. The flow of nitrogen gas was regulated so that the gas pressure in the vicinity of the substrate was approximately 0.67 Pa. Two deposition rates were used: 2.3–3 nm/s without application of the abovementioned beam steering fields, and 20–23 nm/s when the beam steering fields were applied. The deposition duration was 180 s in all cases. The thickness of the coatings was measured by grinding a spherical crater through the coating to the substrate with abrasive slurry applied to a 25.4-mm steel ball, or measured directly in the cross-section scanning electron microscopy (SEM) photographs. A TCI current I up to 40 A was applied during deposition. After the deposition was completed,

the vacuum chamber was backfilled with nitrogen to atmospheric pressure, and the coated bar was removed.

The superficial microhardness was measured with the Vickers indentation test with a load of 25 g. Each data point was an average of 10 measurements. The morphology and composition of the samples were observed using SEM with scattered electrons (SE), backscattered electrons (BSE) and energy dispersive spectroscopy (EDS). X-Ray diffractometry (XRD) characterization was performed with CuKα radiation on a Θ–Θ diffractometer (Scintag), equipped with a liquid nitrogen cooled Ge solid state detector.

3. Results

The thickness of the coatings were ~ 0.4 and ~ 4 μm, respectively, when deposited using the 2.3–3 nm/s and fast 20–23 nm/s deposition rates. Plots of the superficial microhardness of the films as a function of the TCI current are shown in Fig. 2. It may be seen that the microhardness of the thick film was greater then that of the thin film prepared in the absence of TCI. The film microhardness increased with current at relatively small currents ($I < 10$–20 A), then decreased, and then, in the case of the thinner films, increased again with current. The TCI increased the microhardness of the thin films up to a maximum of a factor of 1.7, and the microhardness of the thick films increased up to a factor of 1.3. The maximum microhardnesses of the thick and thin films were obtained at TCI currents of 10 and 20 A, respectively. In general, the superficial microhardness of the thick films were greater than that of the thin films.

XRD patterns of samples with thin coatings showed the substrate material, tungsten carbide (PFD #25-1047). No indication on the existence of any Ti containing phase was observed. The thin films obtained with $I = 0$ and 20 A contain Bragg diffraction lines corresponding to an unknown fcc phase with a lattice

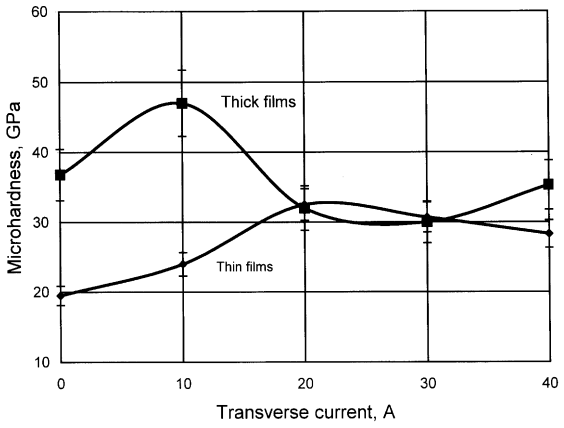

Fig. 2. TiN coating microhardness as a function of injected current.

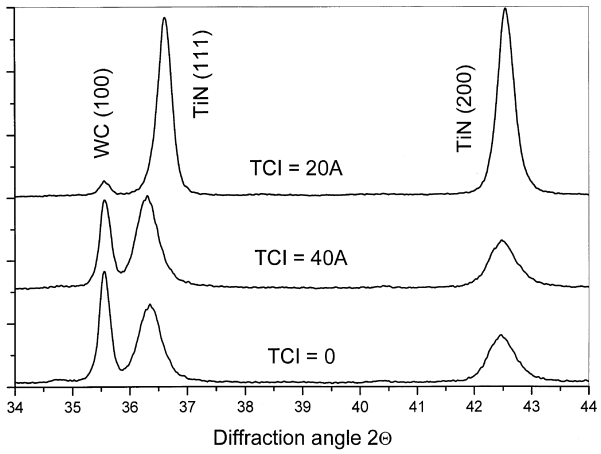

Fig. 3. XRD patterns of thick TiN films for different injected currents.

parameter of 0.4371 nm. XRD patterns of samples with the thick coatings contained Bragg diffraction lines of both the substrate tungsten carbide (PFD #25-1047) and titanium nitride (PDF #38-1420) from the coating (Fig. 3). The XRD data showed that the thick coatings were a cubic NaCl-type TiN phase. The line position and half-width depended on the current. In particular, the shift of positions of the TiN (111) diffraction line to the small angles was observed in the thick coatings obtained without and with TCI of 40 A (Fig. 3).

Fig. 4 shows the BSE images of the thin TiN films deposited on the cemented carbide at $I = 0$ and 40 A. The images contain some bright and dark regions. The regions were distributed uniformly at $I = 0$ (Fig. 4a) while larger bright regions on an almost uniform dark background were observed at $I = 40$ A (Fig. 4b). A completely dark image was obtained at $I = 20$ A. BSE images of the thick TiN films deposited with $I = 0$, 10 and 40 A, respectively, are shown in Fig. 5. The $I = 0$ image consisted of bright regions with various sizes (0.1–1.5 mm) and a non-uniform dark background (Fig. 5a). The $I = 10$ A image consisted of separated larger bright regions (~ 1 mm) on a uniform dark background (Fig. 5b). The $I = 40$ A image consisted of many small bright regions (~ 0.1 mm) on a uniform dark background (Fig. 5c). EDS spectra showed that the dark regions consisted of Ti and N in approximately the same ratio while the bright regions consisted mainly of the virgin cemented carbide. In the thick films, a small amount (~ 10 at.%) of Ti and N was also observed in the bright regions.

4. Discussion

The EDS data indicate that all of the samples contained both Ti and N atoms in approximately the same ratio. Therefore, the absence of Ti-containing phase

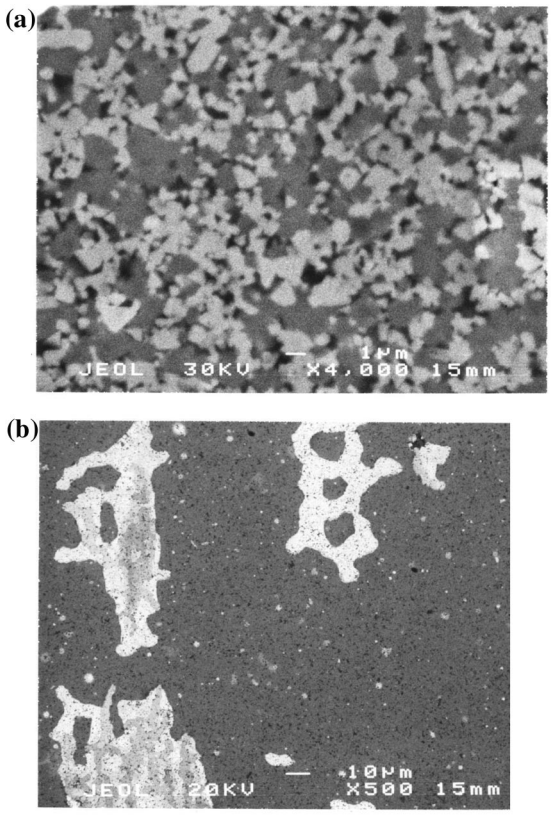

Fig. 4. SEM micrographs (backscattered electrons) of thin TiN films with injected currents: (a) $I = 0$; (b) $I = 40$ A.

lines in the XRD patterns of the thin coatings probably indicates that TiN was present in the films in a nanocrystalline or amorphous form. The unknown FCC phase having a lattice parameter of 0.4371 nm observed in the thin coating with $I = 0$ and 20 A might possibly be tantalum nitride. Ta and Nb compounds closely resemble each other, and fcc δ-niobium nitride has a lattice parameter of 0.4392 nm (PDF #38-1155). This phase may be formed at the initial stages of the deposition from Ta contained in the substrate (approx. 2 at.%).

The speckled BSE images together with the EDS measurements indicate that these low temperature TiN depositions tend to either form imperfectly, i.e. only on portions of the surface, or perhaps delaminate. Thus, portions of the sample surface appear to be bare carbide from the substrate when observed with the SEM. The thin films had much more of these imperfections than the thick films. As a result, without TCI, the microhardness of the thin films was less than that of the thick films and was comparable with the substrate microhardness. The most perfect TiN films were obtained under TCI with $I = 20$ A. This coating was the most continuous, i.e. without what appears to be bare areas. Positions of the Bragg diffraction lines in the thick films completely agree with the reference data (PDF #38-1420), and widths of Bragg diffraction lines were minimal. That means that this sample has the lowest level of microstrain and accordingly the lowest microhardness, and agrees with the microhardness measurements shown in Fig. 2

An interesting feature of the XRD patterns of the thick coatings obtained with TCI of $I = 0$ and 40 A is the shift of positions of TiN (111) diffraction line to the small angles. It means that the lattice parameter calcu-

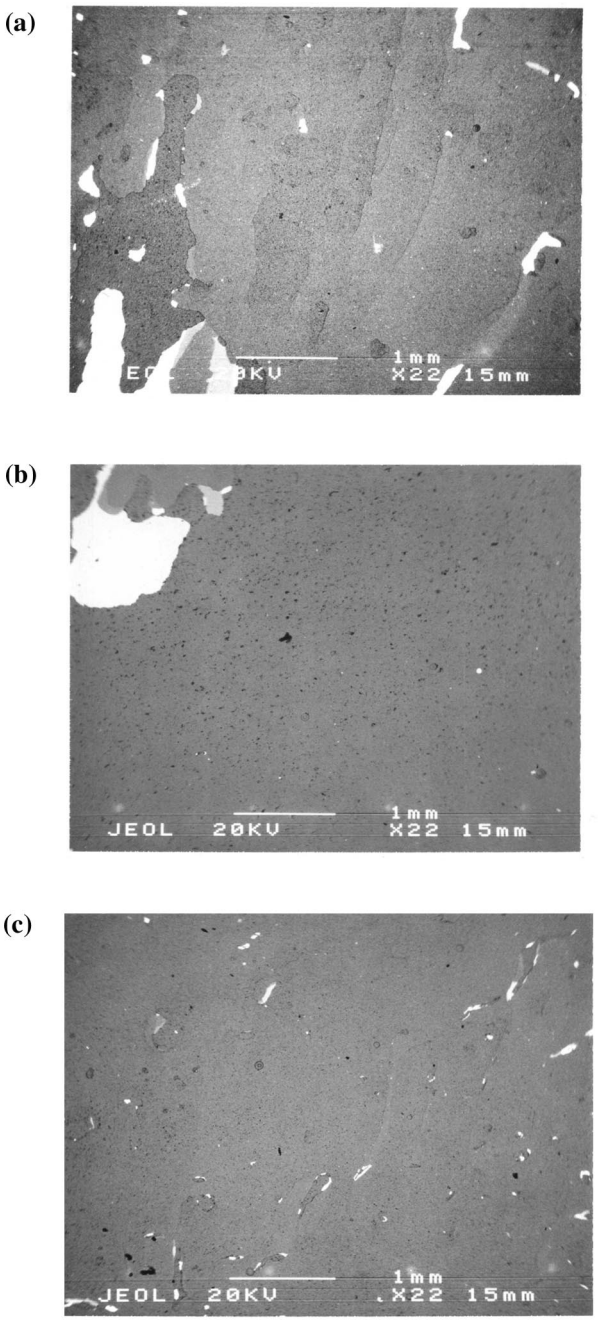

Fig. 5. SEM micrographs (backscattered electrons) of thick TiN films at with injected currents: (a) $I = 0$; (b) $I = 10$; (c) $I = 40$ A.

lated on the basis of lattice spacing from the (111) Bragg peak is substantially greater ($\sim 1\%$) than the lattice parameter calculated on the basis of lattice spacing from other Bragg peaks, for example (200), (220) or (311). This phenomenon has been widely known for approximately 10 years [13–15] however, its unambiguous interpretation is still absent. According to most of the authors the selective entrapment of interstitial atoms and/or selective growth of lattice defects are responsible for the phenomenon observed. Perhaps, both of these reasons may be realized in our case of the low-temperature deposition with TCI.

Adhesion of Ti-N particles on the WC substrate may be insufficient in our case of the low temperature deposition [2,4]. Therefore, the obtained films may be discontinues with high rest stresses. The latter may be the cause of observed delamination of some parts of the film (Fig. 4a). Moreover, hardness is greater for coating with higher levels of residual stresses and smaller grains size [5].

The observed dependencies of the microhardness and the level of the microstrains on the current indicate that the injected current affected the coating structure and state. We can assume that this influence is like knowing the electro-plasticity effect observed at injection of high density current during cold processing of metals [16]. In our case the effect of the current consists of the coating plasticity changing due to influence on state and motion of defects. As a result characteristics of the coating such as adhesion rate, stresses, hardness, etc., are changed. Thus, by using TCI the hard, uniform TiN coating with perfect crystalline structure can be deposited at relatively low temperature.

5. Conclusions

Injection of an electric current into low temperature WC substrates during Ti-N deposition affected the coating properties. The optimal 4 μm coatings were obtained with an injected current density of 0.6 A/mm^2, and had a microhardness of 30–35 GPa, without delamination. Moreover, the following effects were observed:

1. thin (0.3–0.4 μm) Ti-N films deposited at 2.3–3 nm/s had a nanocrystalline or amorphous form, independent of the injected current;
2. thick (3–4 μm) TiN films deposited at 20–23 nm/s had a cubic NaCl-type structure; and
3. the thick films obtained at a current density of 0.6 A/mm^2 had the smallest microstrain.

Additional studies are required to determine the performance characteristics of the TCI-modified films, and to develop techniques for applying TCI in industrial deposition equipment.

References

[1] P.J. Martin, D.R. McKenzie, in: R.L. Boxman, P.J. Martin, D.M. Sanders (Eds.), Handbook of Vacuum Arc Science and Technology, Noyes, Park Ridge, NJ, 1995, p. 467.
[2] A.S. Vereschaka, I.P. Tretyakov, Cutting Tools with Wear Resistant Coatings, Mashinistroenie, Moscow, 1986, pp. 19–38.
[3] V.N. Zhitomirsky, I. Grimberg, R.L. Boxman, B.Z. Weiss, N.A. Travitzky, S. Goldsmith, Surf. Coat. Technol. 94/95 (1997) 206.
[4] E. Erturk, H.J. Heuvel, Thin Solid Films 153 (1987) 135.
[5] M.Y. Al-Jaroudi, H.G.T. Hentzell, Thin Solid Films 154 (1987) 425.
[6] A.J. Perry, J.R. Treglio, A.F. Tian, Surf. Coat. Technol. 76/77 (1995) 815.
[7] A.J. Perry, D.G. Teer, Surf. Coat. Technol. 97 (1997) 244.
[8] N. Parkansky, A. Ben-Shalom, R.L. Boxman, et al. US Patent No. 5.514.229 May 7 1996.
[9] N. Parkansky, R. Rosenbaum, Y. Rosenberg, R.L. Boxman, S. Goldsmith, Surf. Coat. Technol. 76/77 (1995) 197.
[10] N. Parkansky, B. Alterkop, W. Schuster, R.L. Boxman, S. Goldsmith, J. Appl. Phys. 82 (1997) 15.
[11] I. Grinberg, V.N. Zhitomirsky, N. Parkansky et al., Surf. Coat. Technol. 94/95 (1997) 213.
[12] L. Rapoport, A. Rayhel, I. Lapsker, N. Parkansky, R.L. Boxman, S. Goldsmith, J. Mech. Behav. Mater. 9 (1998) 267–276.
[13] I. Goldfarb, J. Pelleg, L. Zevin, N. Croitoru, Thin Solid Films 200 (1991) 117.
[14] A. Laor, L. Zevin, J. Pelleg, N. Croitoru, Thin Solid Films 232 (1993) 143.
[15] F. Elstner, A. Ehrlich, H. Giegengack, H. Kupfer, F. Richter, J. Vac. Sci. Technol. A 12 (1994) 476.
[16] H. Conrad, Mater. Res. Innovat. 2 (1998) 1.